Complexation of Proteins with a Strong Polyanion in an Aqueous Salt-free System

Atsushi Tsuboi,† Tsuyoshi Izumi,† Mitsuo Hirata,† Jiulin Xia,‡ Paul L. Dubin,‡ and Etsuo Kokufuta*,§

Department of Industrial Chemistry, Nihon University, Narashino, Chiba 275, Japan, Department of Chemistry, Indiana-Purdue University, Indianapolis, Indiana 46223, and Institute of Applied Biochemistry, University of Tsukuba, Tsukuba, Ibaraki 305, Japan

Received July 2, 1996. In Final Form: October 7, 1996⊗

We studied the formation in a salt-free solution of complexes between potassium poly(vinyl alcohol) sulfate (KPVS), a strong polyelectrolyte, and proteins with known amino-acid sequences: papain, human serum albumin, lysozyme, ribonuclease, trypsin, and pepsin. Turbidimetric titration, together with quasi-elastic light scattering (QELS), static light scattering (SLS), and electrophoretic light scattering, was performed at pH 2, in order to completely protonate the basic groups of proteins and so facilitate the determination of their total cationic charge. Even at pH 2, no protein unfolding was observed in all the samples within the precision of QELS. Through complexation with KPVS at pH 2, electrically neutral protein−polyelectrolyte complexes (PPCs) with a uniform size were formed from all the proteins, other than pepsin. Such PPCs can be regarded as aggregates of an intrapolymer complex consisting of a KPVS chain with the bound protein molecules, the formation of which occurs via the stoichiometric neutralization of the polyion charges with the opposite charges of proteins. After most of the proteins have formed PPCs, further addition of KPVS led to the association of the aggregated intrapolymer PPCs to form high-ordered aggregates. However, a decrease in the protein charges due to the characteristics of proteins or pH level appears to alter the nature of the PPC formed.

I. Introduction

The complexation of proteins with natural and synthetic polyelectrolytes is interesting from two points of view. The first concerns the way in which the polymers interact with nonflexible protein molecules, an understanding of which could provide a better explanation of the interaction mechanism of polyelectrolytes with ionic colloidal particles. The second concerns the extent to which biochemical activity is maintained in the resulting complexes, the answer to which is central to the molecular design of composite protein−polymer systems, such as immobilized enzymes, as well as to the design of protein separation processes[1] using water-soluble polymers.

A number of studies have dealt with the formation of protein−polyelectrolyte complexes (PPCs) in aqueous salt-free and salt-containing systems under different pH conditions (refs 2−5 as reviews; refs 6−24 as original papers). Turbidimetric titration,[3−5,10−12,17−22] quasi-elastic light scattering (QELS),[4,5,17,19−21,24] static light scattering (SLS),[4−6,9,20] electrophoretic light scattering (ELS)[3−5,19,20,24] and fluorescence spectroscopy[23,24] have been employed. In addition, biochemical methods such as the measurement of enzymatic activity have also been employed in the appropriate cases.[3,5,18,22] The main conclusions derived from these previous studies may be summarized as follows: (i) PPCs are formed mainly through electrostatic forces; (ii) in salt-free systems, at least, protein molecules are complexed with flexible polyelectrolytes through the stoichiometric formation of ion pairs (or salt linkages) between oppositely charged groups;[3,5,10−12,18,22] (iii) the ion pairs between the polyelectrolyte and protein molecules are very labile and may be severed by changes in pH as well as by the addition of small ions and polyions;[3,5,11] and (iv) there is an appreciable retention of biochemical function in the resultant complexes;[3,5,18,22] therefore, changes in the three-dimensional conformations of the protein molecules caused by complexation are not so large as to cause a loss of original functions.

With respect to the process of PPC formation, the previous studies performed in salt-containing systems

* To whom correspondence should be addressed.
† Nihon University.
‡ Indiana-Purdue University.
§ University of Tsukuba.
⊗ Abstract published in *Advance ACS Abstracts,* December 1, 1996.

(1) Dubin, P. L.; Gao, J.; Mattison, K. *Sep. Purif. Methods* **1994**, 23 and references therein.
(2) Dubin, P. L.; Ross, T. D.; Sharma, I.; Yegerlehner, B. In *Ordered Media in Chemical Separations*; Hinze, W. L., Armstrong, D. W., Eds.; American Chemical Society: Washington, DC, 1987; Chapter 8.
(3) Kokufuta, E. In *Macromolecular Complexes in Chemistry and Biology*; Dubin, P. L., Davis, R., Thies, C., Bock, J., Schulz, D., Eds.; Springer-Verlag: Heidelberg, 1993; Chapter 18.
(4) Xia, J.; Dubin, P. L.; Ahmed, L. S.; Kokufuta, E. In *Macro-ion Characterization: From Dilute Solutions to Complex Fluids*; Schmitz, K. S., Ed.; American Chemical Society: Washington, DC, 1994; Chapter 17.
(5) Kokufuta, E.; Dubin, P. L. *Hyomen* **1994**, *32*, 460 (in Japanese).
(6) Nakagaki, M.; Sano, Y. *Bull. Chem. Soc. Jpn.* **1972**, *45*, 1011.
(7) Sternberg, M.; Hershberger, D. *Biochem. Biophys. Acta* **1974**, *342*, 195.
(8) Jendrisak, J. J.; Burgess, R. R. *Biochemistry* **1975**, *14*, 4634.
(9) Sano, Y.; Nakagaki, M. *Nihon Kagaku Kaishi* **1976**, No. 6, 875 (in Japanese).
(10) Kokufuta, E.; Shimizu, H.; Nakamura, I. *Polym. Bull.* **1980**, *2*, 157.
(11) Kokufuta, E.; Shimizu, H.; Nakamura, I. *Macromolecules* **1981**, *14*, 1178.
(12) Kokufuta, E.; Shimizu, H.; Nakamura, I. *Macromolecules* **1982**, *15*, 1618.
(13) Horn, D.; Heuck, C. C. *J. Biol. Chem.* **1983**, *258*, 1665.
(14) Kuznetsova, N. P.; Gudkin, L. R.; Samsonov, G. V. *Vysokomol. Soedin., Ser. A.* **1983**, *25*, 2580.
(15) Kuramoto, N.; Sakamoto, M.; Komiyama, J.; Iijima, T. *Makromol. Chem.* **1984**, *185*, 1419.
(16) Izumurodv, V. A.; Zezin, A. B.; Kabanov, V. A. *Dokl. Akad. Nauk SSSR* **1984**, *275*, 1120.
(17) Dubin, P. L.; Murrell, J. M. *Macromolecules* **1988**, *21*, 2291.
(18) Kokufuta, E.; Takahashi, K. *Polymer* **1990**, *31*, 1177.
(19) Park, J. M.; Muhoberac, B. B.; Dubin, P. L.; Xia, J. *Macromolecules* **1992**, *25*, 290.
(20) Xia, J.; Dubin, P. L.; Dautzenberg, H. *Langmuir* **1993**, *9*, 2015.
(21) Ahmed, L. S.; Xia, J.; Dubin, P. L.; Kokufuta, E. *J. Macromol. Sci., Pure Appl. Chem.* **1994**, *A31*, 17.
(22) Izumi, T.; Hirata, M.; Takahashi, K.; Kokufuta, E. *J. Macromol. Sci., Pure Appl. Chem.* **1994**, *A31*, 39.
(23) Izumi, T.; Hirata, M.; Kokufuta, E.; Cha, H.-J.; Frank, C. W. *J. Macromol. Sci., Pure Appl. Chem.* **1994**, *A31*, 31.
(24) Xia, J.; Dubin, P. L.; Morishima, Y.; Sato, T.; Muhoberac, B. B. *Biopolymers* **1995**, *35*, 411.

S0743-7463(96)00653-1 CCC: $12.00

have proposed that the initial step of the complexation is the formation of "intrapolymer" complexes,[3−5,17,20−24] which may subsequently interact with one another, yielding aggregates or coacervates.[4,5,21] However, only two papers[4,20] provided "direct" evidence for the formation of an intrapolymer PPC by means of SLS in salt solutions. Even if the formal charges of a protein in a salt solution can be determined using appropriate approaches such as potentiometric titration and electrophoresis,[2,5,19−21,24] the data obtained may not be identical with the number of protein charges responsible for the formation of an intrapolymer PPC. The reason is that PPC formation promotes the dissociation of counterions and/or protons; for example,

$$\text{protein-COO}^{-}\,{}^{+}\text{Na} + \text{Cl}^{-}\,{}^{+}\text{N(CH}_3\text{)}_3\text{—}\int \rightarrow \text{protein-COO}^{-}\,{}^{+}\text{N(CH}_3\text{)}_3\text{—}\int + \text{NaCl}$$

and/or

$$\text{protein-COOH} + \text{Cl}^{-}\,{}^{+}\text{N(CH}_3\text{)}_3\text{—}\int \rightarrow \text{protein-COO}^{-}\,{}^{+}\text{N(CH}_3\text{)}_3\text{—}\int + \text{HCl}$$

In fact, it has been demonstrated that the dissociation of counterions and/or protons occurs not only in the formation of PPCs[3,5,11,18] but also in the formation of salt linkages between oppositely charged polyions and colloid particles.[25−27] Therefore, the present study focused on finding a key to understanding the detailed mechanism of PPC formation using a salt-free system.

In a salt-free solution, the formal charge of a protein is equivalent to the number of acidic or basic groups per protein under pH conditions which force to completion their protonation or deprotonation, respectively (usually, pH < 2 and pH > 12.5).[3] Under such pH conditions, many PPCs exhibit 1:1 stoichiometric binding between oppositely charged groups.[3,5,10−12,22] Therefore, the present study employed a salt-free aqueous solution at pH 2 as a medium for PPC formation, except for the study on the effects of protein charge as a function of pH. Potassium poly(vinyl alcohol) sulfate (KPVS) was used as a polyelectrolyte because its net charge remains unchanged over the pH range 2−12 (e.g., see ref 3). Protein samples with known amino-acid sequences were selected; thus, both absolute molecular weight and number of ionizable groups can be determined for each protein, allowing the subsequent calculation of the number of bound protein molecules per KPVS polyion. Consequently, we can estimate *a priori* the molecular weight of each intrapolymer PPC.

Under such strong acidic conditions one may expect a loss in enzyme activity, and in fact, the enzymes used here, other than pepsin, which is a typical acid gastric protease, do not exhibit activities at pH 2. Our previous papers,[3,5,18,22] however, demonstrated an appreciable retention of enzyme activities in PPCs prepared at pH 2. In addition, the present QELS experiments showed that the diameters of the protein samples remain unaltered over the pH range 2−8, indicating no protein unfolding at pH 2.

The turbidimetric titration method was the primary technique used in this study. Since turbidity is known to be proportional to both the molecular weight and the concentration of particles in a system,[28] it can be expected that a detailed comparison of the experimental titration curves with predicted values will provide a good understanding of the complexation mechanism. We also used QELS, SLS, and ELS techniques to obtain information about the size distribution, the molecular weight, and the electric charge of PPCs.

II. Characterization of PPC Formation by Turbidimetric Titration and SLS

Other works have discussed in detail the application to PPC formation of QELS,[4,5,17,19−21,24] SLS,[4−6,9,20] and ELS.[3−5,19,20,24] Here, we attempted to develop a treatment for the turbidimetric titration of the PPC formation process. Related considerations allow us to estimate the molecular weight of PPCs by SLS.

II.1. Turbidimetric Titration. Since turbidity (τ) is proportional to both the molecular weight and the concentration of particles in a system,[28] the process of PPC formation could be studied by monitoring changes in τ during the titration of protein solutions with a polyelectrolyte. The titration of V_i mL of protein solution with V_t mL of polyelectrolyte titrant with a fixed concentration of C_{PE} (in g/mL) gives rise to m_x molecules of PPCs with a weight-average molecular weight ($\bar{M}_x$). τ may then be expressed as

$$\tau = H\bar{M}_x C_x \tag{1}$$

where the proportionality constant (H) and the weight concentration of the PPC (C_x in g/mL) are given by eqs 2 and 3, respectively:

$$H = (32\pi^3/3\lambda_0^4 \boldsymbol{N}_A)\tilde{n}_0^2(\mathrm{d}\tilde{n}/\mathrm{d}c)_x^2 \tag{2}$$

$$C_x = m_x \frac{(\bar{M}_x/\boldsymbol{N}_A)}{(V_t + V_i)} \tag{3}$$

Here, λ_0 is the wavelength of light in a vacuum, $\boldsymbol{N}_A$ is Avogadro's number, $\tilde{n}_0$ is the refractive index of the medium, and $(\mathrm{d}\tilde{n}/\mathrm{d}c)_x$ (in mL/g) is the change in refractive index with PPC concentration.

If only intrapolymer PPC is formed during the titration, then its weight-average molecular weight ($\bar{M}_x^\circ$) may be expressed as

$$\bar{M}_x = \bar{M}_x^\circ = \bar{M}_{PE} + \bar{n}M_{pro} \tag{4}$$

where $\bar{n}$ denotes the average number of bound protein molecules per one polyion chain, $\bar{M}_{PE}$ is the average molecular weight of polyelectrolytes, and M_{pro} is the absolute molecular weight of the proteins. Under this assumption of intrapolymer PPC formation, m_x in eq 3 is equal to the number (m_{PE}) of polyions added into the system. Thus, we can write C_x as

$$C_x = \left(1 + \bar{n}\frac{M_{pro}}{\bar{M}_{PE}}\right)\left(\frac{C_{PE}}{V_i + V_t}\right)V_t \tag{5}$$

Substitution of eqs 4 and 5 into eq 1 gives

$$\tau = H(\bar{M}_{PE} + \bar{n}M_{pro})\left(1 + \bar{n}\frac{M_{pro}}{\bar{M}_{PE}}\right)\left(\frac{C_{PE}}{V_i + V_t}\right)V_t \tag{6}$$

In practice, we measure the absorbance ($A = (\tau l)/2.3$, where

(25) Kokufuta, E.; Hirai, Y.; Nakamura, I. *Makromol. Chem.* **1981**, *182*, 1715.
(26) Kokufuta, E.; Fujii, S.; Nakamura, I. *Makromol. Chem.* **1982**, *183*, 1233.
(27) Kokufuta, E.; Takahashi, K. *Macromolecules* **1986**, *19*, 351.

(28) For example: Flory, P. *Principles of Polymer Chemistry*; Cornell University Press: Ithaca, NY, 1971; pp 287−291.

Table 1. Properties of Protein Samples

protein	M_{pro}[a]	basic groups	isoelectric point	dn/dc (mL/g)[b]	source[c]
papain	23 419	25	8.8−9.5	0.1895	P4762 (papaya latex)
HSA	66 436	100	4.7−5.2	0.1899	A9511 (human serum)
lysozyme	14 306	19	11.0−11.4	0.1951	L6876 (chicken egg white)
ribonuclease	13 682	19	9.5−9.6	0.1925	P5503 (*Aspergillus clavatus*)
trypsin	23 289	20	10.1−10.8	0.1921	P8642 (bovine pancreas)
pepsin	34 488	5	∼2.5	0.1917	P6887 (porcine stomach mucosa)

[a] Calculated on the basis of amino-acid sequence. [b] Determined in 0.01 M HCl (pH 2) with a differential refractometer. [c] See: Sigma Catalog "Biochemicals, Organic Compounds, and Diagnostic Reagents," 1994, Sigma Chemical Co.

l is cell length) under conditions of $V_i \gg V_t$, so eq 6 is more conveniently written as

$$A = H\left(\frac{l}{2.3}\right)\left(\frac{C_{PE}}{V_i}\right)\left\{\bar{M}_{PE} + \left(2\bar{n} + \frac{\bar{n}^2 M_{pro}}{\bar{M}_{PE}}\right)M_{pro}\right\}V_t \quad (7)$$

If $\bar{n}$ is constant with V_t, then $A = (\text{constant})V_t$. As noted above, complexes formed in a salt-free solution are stoichiometric, corresponding to constant $\bar{n}$. Therefore, $\bar{n}$ may be obtained from the slope of A vs V_t. If complexes are indeed intrapolymer and electrically neutral, then $\bar{n}Z_{pro} = Z_{PE}$, where Z_{pro} and Z_{PE} are the net charges of protein and polyion, respectively. Thus, $\bar{n} = Z_{PE}/Z_{pro}$, i.e., the degree of polymerization divided by the number of protein basic groups in this case. Consequently, one may test this hypothesis by comparing Z_{PE}/Z_{pro} to the value of $\bar{n}$ obtained from the measured dA/dV_t, in connection with eq 7.

II.2. SLS. $\bar{M}_x$ and the root mean square of gyration (R_g^2) for the PPC may be estimated by SLS using the following equation:

$$\frac{KC_x}{R_\theta} = \frac{1}{\bar{M}_x}\left(1 + \frac{16\pi^2}{3\lambda^2}R_g{}^2 \sin^2\frac{\theta}{2}\right) + 2A_2C_x \quad (8)$$

Here, R_θ is the Rayleigh ratio, θ is the scattering angle, λ ($=\lambda_0/\tilde{n}_0$) is the wavelength of the light in the medium, A_2 is the second virial coefficient, and K is given as

$$K = (2\pi^2/\lambda_0^4 \boldsymbol{N}_A)\tilde{n}_0^2(\mathrm{d}\tilde{n}/\mathrm{d}c)_x^2 \quad (9)$$

Therefore, we can obtain both $\bar{M}_x$ and R_g from eq 8 if (d$\tilde{n}$/dc)$_x$ is known. This value was determined in the same way as in the previous studies[4,20] using the following equation:

$$\left(\frac{\mathrm{d}\tilde{n}}{\mathrm{d}c}\right)_x = \frac{1}{1+\beta}\left(\frac{\mathrm{d}\tilde{n}}{\mathrm{d}c}\right)_{PE} + \frac{\beta}{1+\beta}\left(\frac{\mathrm{d}\tilde{n}}{\mathrm{d}c}\right)_{pro} \quad (10)$$

where (d$\tilde{n}$/dc)$_{PE}$ and (d$\tilde{n}$/dc)$_{pro}$ are a change in refractive index with concentration for polyelectrolyte and protein, respectively, and β represents the mass ratio of bound protein to polymer, which can be expressed as

$$\beta = \bar{n}\frac{M_{pro}}{\bar{M}_{PE}} \quad (11)$$

As a result, it was found that SLS is also useful for determining $\bar{M}_x$ and R_g in the present case.

III. Experimental Section

III.1. Materials. The proteins used here are listed in Table 1. Since their amino-acid sequences are known, the number of ionizable groups and the absolute molecular weight (M_{pro}) could be determined for each. Potassium poly(vinyl alcohol) sulfate (KPVS; degree of esterification = 0.922; equivalent weight = 166) was used as the polyelectrolyte; its weight-average molecular weight ($\bar{M}_w$) was found to be 1.89×10^5 from SLS measurements in a 0.2 M NaCl solution. A salt-free solution at pH 2 (0.01 M HCl) was employed as a medium in this study, except for the study on the effects of protein charge as a function of pH. In the latter case, a solution of 0.01 M NaCl with a desired pH was prepared by the addition of 0.1 M HCl or 0.1 M NaOH. All water was deionized, distilled, and filtered through a Gelman 0.2 μm filter.

III.2. Turbidimetric Titration. Salt-free aqueous sample solutions (30 mL) with a fixed protein concentration were titrated at 25 °C in a cubic 2.6 cm path length glass cell with a KPVS solution as the titrant, using an automatic recording titrator (Hirama Model ART-3). The absorbance (A) at 460 nm was automatically recorded as a function of titrant volume during the course of the titration. Unless otherwise noted, the concentrations of protein and KPVS were 0.1 and 0.415 mg/mL, respectively. In order to avoid changes in pH during titration, both protein and polyelectrolyte solutions were adjusted to the same pH level.

III.3. QELS. A Brookhaven system (Holtsville, NY) equipped with a 256-channel digital autocorrelator (BI-2030 AT) and a 2 W Ar laser (Stabilite 2017, Spectra-Physics Lasers) was used in QELS experiments. Unless otherwise stated, all the measurements were performed at a scattering angle of 90°. A 400 μm pinhole aperture was used for the EMI photomultiplier tube, and decalin (decahydronaphthalene) was used as the refractive index matching fluid to reduce stray light. We utilized the homodyne intensity−intensity correlation function $G(q,t)$, with the amplitude of the scattering vector (q) given by

$$q = (4\pi\tilde{n}_0/\lambda_0)\sin(\theta/2) \quad (12)$$

For a Gaussian distribution of the intensity profile of the scattered light, $G(q,t)$ is related to the electric field correlation function $g(q,t)$ by

$$G(q,t) = B[1 + bg(q,t)^2] \quad (13)$$

where B is the experimental baseline and b is a constant depending on the number of coherence areas generating the signal ($0 < b < 1$). The quality of the measurements was verified by determining that the difference between the measured and calculated B values was less than 1% (it was possible to complete our measurements within 1 min due to the power of the laser used). The electric field correlation function depends on the Fourier transform of the fluctuating number density of particles or molecules. For the center of mass diffusion of identical particles, the following simple relation holds:

$$g(q,t) = \mathrm{e}^{-t/\tau} \quad \text{and} \quad (1/\tau) = Dq^2 \quad (14)$$

where τ is the decay time and D is the diffusion coefficient.

For polydisperse systems, the correlation function can be expressed as an integral of the exponential decays weighted over the distribution of relaxation times $\rho(\tau)$:

$$g(t) = \int_0^\infty \mathrm{e}^{-t/\tau}\rho(\tau)\,\mathrm{d}\tau \quad (15)$$

In principle, it is possible to obtain the distribution $\rho(\tau)$ by integral transformation of the experimental $[G(t)/B - 1]^{1/2}$, but in practice this presents a formidable problem for numerical analysis, since taking the inverse Laplace transform is numerically an ill-posed problem. Several numerical methods developed to date are

devoted to calculating $\rho(\tau)$. Here, we analyze the autocorrelation functions using the CONTIN program (see ref 29).

From eq 15, the mean relaxation time, $\langle\tau\rangle$, defined as the area of $g(t)$, is given by

$$\langle\tau\rangle = \int_0^\infty g(t)\,dt = \int_0^\infty \tau\rho(\tau)\,d\tau \Big/ \int_0^\infty \rho(\tau)\,d\tau \qquad (16)$$

This $\langle\tau\rangle$ value can be resolved from each of the distribution modes of $\rho(\tau)$, as the first moment of the normalized relaxation spectrum. Therefore, the diffusion coefficient, which corresponds to each value of $\langle\tau\rangle$, can be calculated using

$$D = \lambda^2/[16\pi^2 \sin^2(\theta/2)\langle\tau\rangle] \qquad (17)$$

From each D value we obtain the Stokes diameter, d_s, using the Einstein equation,

$$d_s = 2\left(\frac{kT}{6\pi\eta D}\right) \qquad (18)$$

where k is the Boltzmann constant, T is the absolute temperature, and η is the viscosity of the solvent. In the present study, the experimental uncertainty is less than 5%.

III.4. SLS. The same Brookhaven system as described above was used for SLS measurements. The calibration was made by using pure (>99.5%) toluene, and the optical alignment was ensured by less than 3% deviation from linearity in the $I \sin\theta$ vs θ plot over the range $45 \le \theta \le 150$. Each measurement was carried out for 1 s. On the basis of the average of five such measurements, we determined the R_θ values. Concentrations of free protein reference solutions (pH 2.0) were determined according to the predicted number of bound proteins, discussed later.

In order to calculate the value of $(d\tilde{n}/dc)_x$ from eq 10, $(d\tilde{n}/dc)_{PE}$ and $(d\tilde{n}/dc)_{pro}$ were measured at 25 °C using an Otsuka electrophotometric differential refractometer (model DRM-1021). The measurements were carried out using unpolarized light from an iodine arc with a spectrum filter whose wavelength was 488 nm. The instrument constant was obtained by using a standard KCl solution (0.01481 g/mL) with a known $d\tilde{n}/dc$ value of 0.1344.

III.5. ELS. The measurements were made at a fixed scattering angle of 8.7° using a Coulter DELSA 400 apparatus (Hialeah, FL). The electric field was applied at a constant current of 0.3 mA. The temperature of the thermostated chamber was maintained at 25 °C. The principle used in determining the electrophoretic mobility has been described in detail in a previous paper (e.g., see ref 4). The mobilities obtained in this work were repeatable to within less than 5%.

IV. Results and Discussion

IV.1. Effect of pH on Unfolding of Protein Samples. The use of a low pH simplifies the analysis of protein charge, in which Z_{pro} = number of basic residues. However, the elucidation of the PPC structure could be complicated by protein unfolding. Therefore, we examined the pH dependence of d_s for all the protein samples by means of QELS. The results obtained are shown in Table 2, together with hydrodynamic diameters (d_h), which were calculated by

$$d_h = 2\left(\frac{f}{f_{min}}\right)\left(\frac{3\bar{\nu}M_{pro}}{4\pi\boldsymbol{N}_A}\right)^{1/3} \qquad (19)$$

using the partial specific volume ($\bar{\nu}$) and the frictional ratio (f/f_{min}). Here, f represents the actual frictional coefficient, and f_{min} is the minimum frictional coefficient for a hypothetical sphere. Both $\bar{\nu}$ and f/f_{min} have been experimentally determined for various proteins and collected in several data books (e.g., see ref 30). As can be seen from Table 2, there is no change in d_s with pH for each protein sample within the precision of QELS; this conclusion is also supported by the fact that d_s agrees with d_h. Therefore, we concluded that the native structure is not seriously perturbed by the low pH condition.

Table 2. pH Changes of d_s for Protein Samples

protein	d_s (nm) pH 8	pH 4	pH 3	pH 2	$\bar{\nu}^a$	$f/f_{min}{}^a$	d_h (nm)^b
papain	4.1		4.3	4.2	0.72	1.16	4.4
HSA		7.2	7.0	7.3	0.73	1.31	7.0
lysozyme	3.9		4.0	3.9	0.72	1.21	3.9
ribonuclease	3.8		3.9	3.9	0.70	1.24	3.9
trypsin	4.8		4.5	4.8	0.75	1.20	4.6
pepsin	4.7		4.8	4.8	0.74	1.11	4.8

[a] Shows the literature values determined at 20 °C (see ref 30). [b] Calculated by introducing $\bar{\nu}$, f/f_{min}, and M_{pro} (see Table 1) into eq 19.

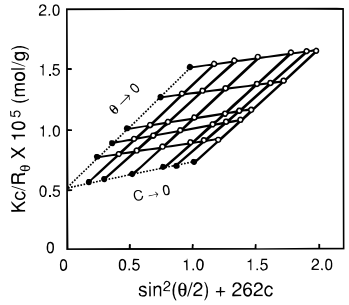

Figure 1. Zimm plots for KPVS in 0.2 M NaCl solution. C_{PE} = 1−4 (mg/mL); θ = 45−150°.

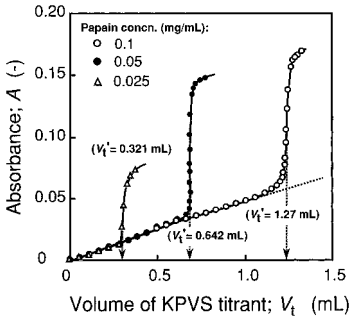

Figure 2. Turbidimetric titration curves of papain solutions (30 mL) with different concentrations of KPVS. C_{PE} = 0.415 mg/mL, which is equivalent to 2.5×10^{-3} mol/L in molar concentration based on the ionizable groups.

IV.2. Properties of KPVS. SLS measurements for KPVS were carried out in 0.2 M NaCl. The $d\tilde{n}/dc$ for this solvent was found to be 0.097 37 mL/g. Figure 1 shows the Zimm plots, from which we obtained $\bar{M}_w = 1.89 \times 10^5$, R_g = 31 nm, and second virial coefficient = 1.27×10^{-3} cm^3 mol/g^2. In addition, the hydrodynamic radius (R_h) for KPVS in 0.2 M NaCl was estimated to be 12 nm by QELS.

IV.3. Turbidimetric Titration Curves. Figure 2 shows typical titration curves of papain with KPVS, from which two important characteristics are observed: (i) Absorbance increases linearly with an increase in V_t and it increases abruptly at V_t'; the value of V_t' is a linear function of papain concentration. (ii) At $V_t < V_t'$ the slopes of each line are independent of papain concentration (the linearity of $A(V_t)$ was also confirmed by the fact that the differential plots of $\Delta A/\Delta V_t'$ vs V_t showed no significant deviation from a constant value at $V_t/V_t' < 0.75$).

(29) We also employed the method of cumulants for analyzing the autocorrelation functions throughout all the QELS measurements other than those for pepsin at $V_t/V_t' \le 0.25$ (where V_t' is the titrant volume at the end point). The diffusion coefficients from the cumulants method and from the CONTIN program agreed within the precision of QELS (5%).

(30) For example: Dayhoff, M. O. *Atlas of Protein Sequence and Structure*; National Biomedical Foundation: Washington, DC, 1972.

Table 3. Comparison of the Number of Cationic Charges per Unit Mass of Protein (N_c) Obtained from Turbidimetric Titrations and Calculated from the Number of Basic Groups

protein	N_c at pH 2 (mequiv/g) obsd[a]	calcd[b]
papain	1.05_8 (1.27)	1.068
HSA	1.50_8 (1.81)	1.505
lysozyme	1.32_5 (1.59)	1.328
ribonuclease	1.35_8 (1.63)	1.381
trypsin	0.85_8 (1.03)	0.860
pepsin	0.14_2 (0.17)	0.145

[a] Determined from V_t' of the KPVS titrant with $C_{PE} = 0.415$ mg/mL for the titrations of 30 mL of sample solutions containing 3 mg of proteins; the V_t' values were shown in parentheses. [b] Calculated by dividing the number of basic groups by M_{pro} for each protein.

In a previous study,[22] we measured the concentration of free papain remaining in the titration system as a function of V_t using the absorbance (280 nm) of the supernatant solutions from which the PPC had been separated by centrifugation. It was found that the free papain concentration decreases linearly with increasing V_t and becomes zero at $V_t \geq V_t'$. Therefore, this characteristic V_t' value can be viewed as the end point of the titration. This result is also evidence that the binding constant for complex formation under these conditions is very large.

Assuming stoichiometric electroneutrality in the complex, the number of cationic charges per unit mass of protein (N_c in mequiv/g) was calculated from V_t' using the following equation:

$$N_c = 10^3(C_{PE}V_t/M°)/(C_{pro}V_i) \qquad (20)$$

where $M°$ is the molecular weight per ionizable group (i.e., equivalent weight) for KPVS, C_{pro} is the protein concentration (g/mL), and V_i is the initial volume (mL) of the sample solution. The N_c obtained was compared with that determined from the number of basic groups in Table 1. As can be seen from Table 3, there is an excellent agreement between N_c from V_t' and that from the number of basic groups. This indicates that the protein molecule forms a PPC with KPVS through a 1:1 stoichiometric binding between oppositely charged groups; i.e., $\bar{n}Z_{pro} = Z_{PE}$.

We observed linearity of $A(V_t)$ at $V_t < V_t'$ in the titration curves for all of the proteins, except for pepsin (the details of the results for pepsin will be discussed later). This observation is consistent with the prediction in the previous section and may be said to reflect an increase in the concentration of PPCs formed during the course of the titration, at constant molecular weight.

IV.4. Examination of the Titration Process by QELS. The binding of proteins to KPVS ions is quite strong, as there is essentially no free polyion in our systems for $V_t \leq V_t'$. Previous QELS studies[4,5,17,19−21,24] have demonstrated that, since the contribution of free proteins to the scattering signal is essentially negligible, only PPC particles were detectable. The titration processes were examined by QELS in order to investigate the size of the PPCs formed. QELS measurements were thus carried out under the same conditions as those used in the titration. Our preliminary experiments showed that reproducible QELS data can be obtained when the measurement is performed within at least 1 day after the sample preparation throughout the titration of protein with KPVS.

Figure 3 shows the results for HSA as a typical example. There was little difference in the apparent distributions

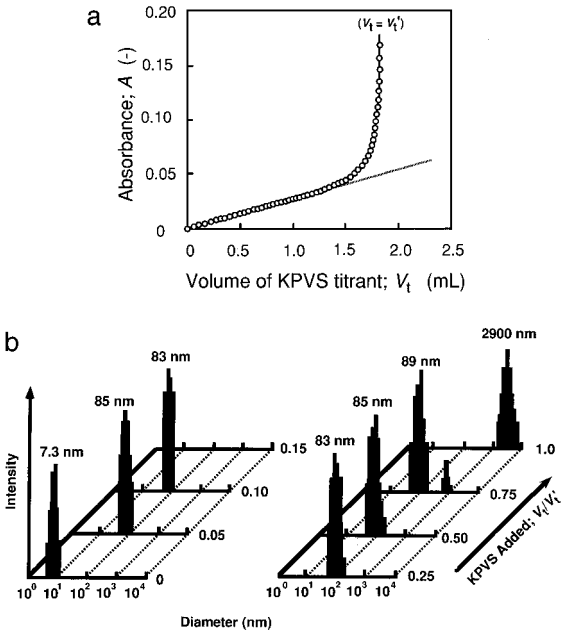

Figure 3. Changes in absorbance (a) and apparent distributions of Stokes diameter (b) due to PPCs formed during the course of turbidimetric titration for a sample solution (30 mL; pH 2) containing 3 mg of HSA with KPVS titrant ($C_{PE} = 0.415$ mg/mL). In part b the amount of KPVS added was given by V_t/V_t'; $V_t' = 1.81$ mL. The values for diameter in the figure denote 100% of the intensity-weighted distribution value.

of d_s for PPCs as well as in the average Stokes diameter ($\bar{d}_s$) until $V_t/V_t' = 0.75$. At $V_t/V_t' = 1$, however, very large particles of PPC ($\bar{d}_s \cong 3000$ nm) were observed. These results are in conformity with the previous interpretation of the turbidimetric titration curve: a linear increase in A with V_t at $V_t < V_t'$ is due to an increase in the PPC concentration at constant PPC size, followed by a very rapid increase in A at $V_t = V_t'$, associated with an increase in PPC size due to aggregation. Similar results were observed for all the proteins in this study, except for pepsin (see Table 4).

In the case of pepsin, the results of the titration and QELS were markedly different from those for the other proteins. As shown in Figure 4a, the titration curve displays a rapid increase for $V_t < V_t'$, a maximum at $V_t = V_t'$, and then a gradual decrease for $V_t > V_t'$. The results of QELS in Figure 4b show the formation of two PPC species: a big particle with $\bar{d}_s \sim 1300$ which is observed only in the range of $V_t/V_t' \leq 0.25$ and a small particle whose size ($\bar{d}_s \sim 280$ nm) is kept almost constant over the range $V_t/V_t' \leq 1$ but gradually decreases at $V_t/V_t' > 1$. To explain these results, we note the very small number of the basic groups (Table 1) or a very low N_c of cationic charges (Table 3) for pepsin. Consequently, 228 protein molecules are required to neutralize one polyion. This causes a very high flexibility in the bound proteins within the resultant PPC. As a result, pepsin seems to be distinct from the other proteins with regard to complexation with KPVS.

The results for pepsin suggest that the number of charged groups per protein molecule may influence the size of the PPCs formed during the course of the titration. It was thus predicted that the reduction of cationic protein charges by increasing pH for proteins other than pepsin, e.g., lysozyme, would produce a similar result. In order to confirm this prediction, the complexation of lysozyme with KPVS was examined as a function of pH using turbidimetric titration and QELS. As can be seen from Figure 5, the slope of the titration curve obtained increased with an increase in pH. In particular, at pH 11—near the isoelectric point—the titration curve displays a maximum

Table 4. Values of $\bar{d}_s$ Obtained in the Course of Turbidimetric Titration[a]

protein	$\bar{d}_s$ (nm) for the following values of KPVS added, V_t/V_t'					
	0.05	0.10	0.25	0.50	0.75	1.0
papain	100	100	100	100	140	2100
HSA	85	83 ± 2[b]	84 ± 1[b]	85 ± 1[b]	89	2900
lysozyme	99	100	100	100	110	2200
ribonuclease	71	68	66	64	87	1600
trypsin	120	120	120	120	120	3700
pepsin	(260; ca. 1300)[c]	(280; ca. 1300)[c]	(280; ca. 1300)[c]	280	280	280

[a] Titrations were conducted under the same conditions as shown in Table 3, except that the concentration of KPVS titrant used for pepsin was one-tenth the titrant concentration for the other proteins (see Figure 4). [b] Determined at three different angles (60, 90, and 120°). [c] Two species with different sizes were detected.

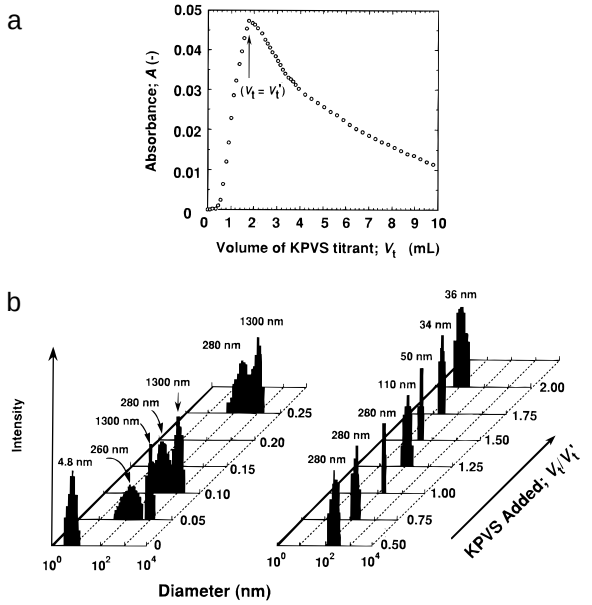

Figure 4. Changes in absorbance (a) and apparent distributions of Stokes diameters (b) during the course of turbidimetric titration for a sample solution (30 mL; pH 2) containing 3 mg of pepsin with KPVS titrant (C_{PE} = 0.0415 mg/mL). Because of the low charge of pepsin, the titrant concentration was reduced to one-tenth of that used for the other proteins; thus, the obtained V_t' value was 1.73 mL.

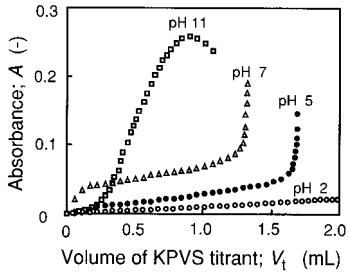

Figure 5. Turbidimetric titration curves of lysozyme with KPVS at different pHs. Sample solutions (30 mL) containing 3 mg of protein were titrated with a KPVS solution (C_{PE} = 0.208 mg/mL), the concentration of which is equivalent to 1.25 × 10^{-3} mol/L on the basis of the ionizable groups and equal to half the titrant concentration commonly employed in this study. The V_t' values (in mL) obtained as a function of pH were 3.18 (pH 2); 1.69 (pH 5); 1.32 (pH 7); and 0.91 (pH 11).

similar to that of pepsin. These results may be interpreted according to eq 7, in which the slope of the turbidimetric titration curve is seen to depend only on $\bar{n}$, which is thus found to increase with pH. These findings agree with the QELS results shown in Figure 6. We observed an increase in PPC size with pH, which may also be explained by an increase in $\bar{n}$ with pH, as can be predicted from eq 7. In addition, it was found that large PPC particles appear in the initial stage of the titration at pH > 7 and at $V_t/V_t' \leq$ 0.25, together with the particles with a constant size for $V_t/V_t' < 0.8$. This finding agrees with the results for pepsin shown in Figure 4b.

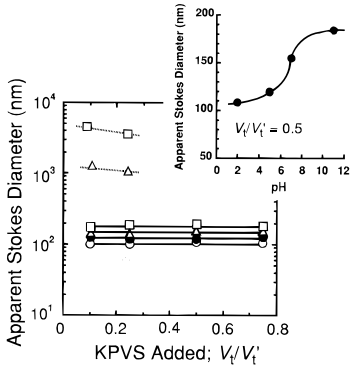

Figure 6. Changes in apparent Stokes diameter for lysozyme–KPVS complexes formed during the course of turbidimetric titrations at different pHs: (○) 2; (●) 5; (△) 7; (□) 11. The amount of KPVS added was normalized by V_t/V_t' using the V_t' values at different pHs (see Figure 5).

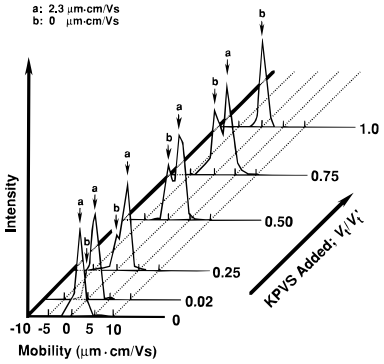

Figure 7. Change in electrophoretic mobility during the course of turbidimetric titration of HSA with KPVS at pH 2. The conditions used for the titration were the same as those described in Figure 3.

IV.5. Examination of the Complexation by ELS. We also employed the ELS technique for the examination of the titration processes. Figure 7 shows ELS spectral changes during the course of the titration of HSA with KPVS as a typical example. Free HSA molecules at pH 2 exhibited a peak in electrophoretic mobility (U) at 2.30 μm·cm/V·s, while the addition of KPVS gave rise to a second peak at $U = 0$ μm·cm/V·s, with the peak due to free HSA disappearing completely at $V_t/V_t' = 1$. This result clearly demonstrates that the HSA–KPVS complex is electrically neutral. The same conclusion was drawn from the ELS spectra for the other proteins, except for pepsin.

In the case of pepsin, the formation of an electrically neutral PPC at the end point of the titration was evidenced by the appearance of a peak at $U = 0$ μm·cm/V·s at $V_t/V_t' = 1$ (see Figure 8). This is consistent with the results in Table 3, demonstrating that, even in the case of pepsin,

Table 5. Comparison of Observed and Calculated Slopes of Turbidimetric Titration Curves

protein	β	$(d\tilde{n}/dc)_x$ (mL/g)	$10^6 H$ (cm^2/g^2)	$\bar{n}$	$10^{-6}\left\{\bar{M}_{PE}+\left(2\bar{n}+\frac{\bar{n}^2M_{pro}}{\bar{M}_{PE}}\right)M_{pro}\right\}$ (g)	$10^2\left(\frac{dA}{dV_t}\right)_{obsd}$ (mL^{-1})	$10^4\left(\frac{dA}{dV_t}\right)_{calcd}$ (mL^{-1})	$10^2\alpha\left(\frac{dA}{dV_t}\right)_{calcd}$ (mL^{-1})
papain	5.6	0.1756	6.685	46	8.35	5.15	8.72	4.71
HSA	4.0	0.1714	6.367	11	4.73	2.62	4.71	2.12
lysozyme	4.5	0.1775	6.824	60	5.80	3.72	6.18	3.96
ribonuclease	4.3	0.1747	6.613	60	5.39	0.32	5.57	0.39
trypsin	7.0	0.1803	7.044	57	12.1	7.05	13.4	6.96

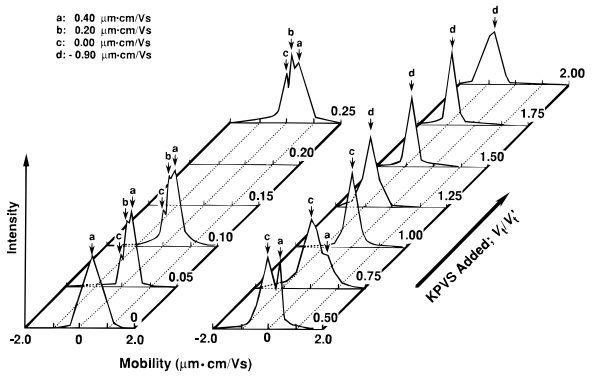

Figure 8. Change in electrophoretic mobility during the course of turbidimetric titration of pepsin with KPVS at pH 2. The conditions used for the titration were the same as those described in Figure 4. Peaks a and b in the spectra at $V_t/V_t' =$ 0.05, 0.1, and 0.25 are very close; however, the mobilities corresponding to these peaks were reproduced to within less than 5% for triplicate measurements with different samples.

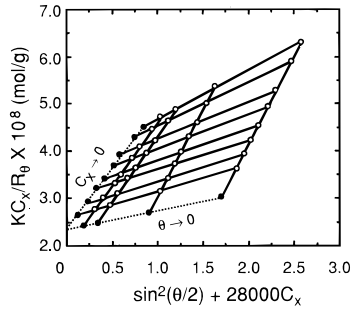

Figure 9. Zimm plots for PPC consisting of HSA and KPVS at pH 2.0. $C_x = 6.30 \times 10^{-6}$ to 6.11×10^{-5} g/mL, which was estimated using eq 5; $\theta = 45-135°$. The estimated second virial coefficient, 5.56×10^{-5} cm^3 mol/g^2, is negligibly small.

there is a good agreement between the observed and calculated cationic charges (stoichiometric complexation). In the initial stage of the titration, however, a peak at $U = 0.20\ \mu$m·cm/V·s appeared in the ELS spectra, in addition to the peaks due to free pepsin ($U = 0.40\ \mu$m·cm/V·s) and neutral PPC ($U = 0\ \mu$m·cm/V·s). Because the results of QELS in Figure 4b showed that two species of PPCs with different sizes are formed in the initial stage of the titration, this peak may be assigned to the large particles with $\bar{d}_s \sim 1300$, presumably formed through the association of positively charged free proteins with the neutral PPC particles with $\bar{d}_s \sim 280$ nm. It appears that the subsequently added KPVS ion takes off the associated proteins from the large PPCs and forms a neutral PPC. Therefore, we observed only the neutral particle with a uniform size (ca. 280 nm) in the range $0.25 < V_t/V_t' < 1.0$ (it should be noted that free pepsin can be detected by ELS but not by QELS).

Another important finding in Figure 8 is that, at $V_t/V_t' > 1$, negatively charged particles with $U = -0.9\ \mu$m·cm/V·s are detected by ELS. Since the free KPVS ion exhibited a mobility of $-2.0\ \mu$m·cm/V·s under the conditions used, such particles can be regarded as a PPC with negative charges. As was mentioned in the previous section, 228 molecules of pepsin would be required for complete neutralization of the negative charges of a KPVS ion. Thus, the neutral PPC detected by ELS seems to contain many of the pepsin molecules which are loosely linked with the polyion. By adding excess KPVS, such weakly bound proteins give rise to a new PPC with negative charges, and at the same time the neutral PPC turns into another negative PPC particle. Consequently, KPVS addition over $V_t/V_t' > 1$ leads to a decrease in the size of PPCs as shown in Figure 4b. As a result, we believe that pepsin is distinct from the other proteins with regard to the PPC formation mechanism (the details will be discussed later).

IV.6. Quantitative Analyses of the Titration Curves. All of the proteins other than pepsin show evidence of the formation of an electrically neutral PPC with a uniform size. We attempted to clarify the nature of such a complex through a quantitative analysis of the titration data. From eq 7, the slope (dA/dV_t in mL^{-1}) of titration curves at $V_t < V_t'$ can be expressed as

$$dA/dV_t = H\left(\frac{l}{2.3}\right)\left(\frac{C_{PE}}{V_i}\right)\left\{\bar{M}_{PE}+\left(2\bar{n}+\frac{\bar{n}^2M_{pro}}{\bar{M}_{PE}}\right)M_{pro}\right\} \quad (21)$$

Since $(d\tilde{n}/dc)_x$ in eq 2 may be approximated by introducing the measured $(d\tilde{n}/dc)_{PE}$ and $(d\tilde{n}/dc)_{pro}$ values into eq 10, we can determine all the terms in eq 21 and calculate dA/dV_t for each sample, assuming only intrapolymer complexes. The calculated slopes are shown in Table 5, together with other required quantities in the calculation. The observed values are 6−60 times larger than the calculated ones. This result suggests the possibility of multipolymer aggregates with a uniform size, for which $\bar{M}_x = \alpha\bar{M}_x^\circ = \alpha(\bar{M}_{PE} + \bar{n}M_{pro})$, where α is the degree of aggregation, i.e., the number of polymer chains within one complex. To evaluate α, we carried out SLS experiments under the same conditions as those used in the titration and QELS experiments.

IV.7. Estimations of Molecular Weight and Degree of Aggregation by SLS. For a multipolymer aggregate of intrapolymer complexes, we simply can rewrite $\bar{M}_x$ in eq 8 as $\alpha\bar{M}_x^\circ$. However, regardless of α, C_x is given by eq 5; i.e., $C_x = C_p(1 + \beta)$, where $C_p = \{C_{PE}/(V_i + V_t)\}V_t$ and $\beta = \bar{n}(M_{pro}/\bar{M}_{PE}) = (Z_{PE}/Z_{pro})(M_{pro}/\bar{M}_{PE})$. Therefore, using eq 8, we can estimate $\bar{M}_x$ (i.e., $\alpha\bar{M}_x^\circ$) from the analysis of SLS data.

The angular dependence of scattered light was determined as a function of C_x, which was calculated from V_t using eq 5. Figure 9 shows a typical Zimm plot for HSA obtained at $\theta = 45-135°$ and at $C_x = 6.30 \times 10^{-6}$ to 6.11×10^{-5} g/mL. For all protein samples other than pepsin, the double extrapolations of KC_x/R_θ vs $(\sin^2(\theta/2) + kC_x)$ plots to $\theta \to 0$, and $C_x \to 0$ also gave two straight lines with correlation coefficients > 0.99, cointersecting the Y axis, enabling us to determine $\bar{M}_x$ and R_g. These results are listed in Table 6, together with α and $\bar{M}_x^\circ$. It is found that

Table 6. Results of SLS

protein	$\bar{M}_x^{\circ}$ [a]	$\bar{M}_x$	α [b]	R_g	ρ (=R_g/R_h)
papain	1.26×10^6	7.36×10^7	54	69	1.3_8
HSA	9.46×10^5	4.28×10^7	45	53	1.2_6
lysozyme	1.05×10^6	6.67×10^7	64	79	1.5_8
ribonuclease	1.01×10^6	6.64×10^6	7	37	1.0_9
trypsin	1.51×10^6	7.84×10^7	52	80	1.3_3

[a] Calculated by eq 4. [b] Determined by $\alpha = \bar{M}_x/\bar{M}_x^{\circ}$.

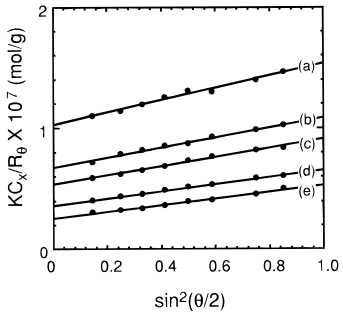

Figure 10. Plots of KC_x/P_θ vs $\sin^2(\theta/2)$ for HSA−KPVS complexes as a function of C_x ($\times 10^{-6}$ g/mL): (a) 3.67; (b) 2.46: (c) 1.85; (d) 1.24; (e) 0.62. Each PPC sample was prepared by the titration of HSA with KPVS under the same conditions used in Figure 3; therefore, C_x corresponds to the following V_t/V_t': (a) 0.03; (b) 0.02; (c) 0.015; (d) 0.01; (e) 0.005.

the $\bar{M}_x$ values obtained are much larger than M_x°, leading to α ranging from 45 to 64 for all the proteins, except for ribonuclease, for which α is much smaller than that observed for the other proteins.

To compare SLS results with turbidimetric titration curves, we introduce the term α into the right-hand side of eq 7. Thus, from α and $\bar{n}$, we may calculate the expected turbidimetric slope dA/dV_t. This calculated slope is compared to the measured value in Table 5. The good agreement seen in columns 7 and 9 of Table 5 supports the hypothesis that a multipolymer aggregate of intrapolymer PPCs forms during the course of the titration at $V_t < V_t'$.

From the results of SLS and from the $\bar{d}_s$ values in Table 4, we obtain $\rho = R_g/R_h$ for aggregates of intrapolymer PPCs. Hydrodynamic theory[31] shows that ρ changes from infinity to 0.775 when the polymer structure changes from a long rod to a sphere, with values from 1.3 to 1.5 for random coils. As can be seen from Table 6, ρ ranges from 1.1 to 1.6. This result may lead to a question as to why electrically neutral aggregates of intrapolymer PPCs do not form compact spherical structures. The binding of many protein molecules to an extended polymer chain may prevent the complex from adopting a fully collapsed configuration because of a steric repulsion among bound proteins (see next section).

IV.8. Trials to Detect Intrapolymer PPCs by SLS and QELS. In order to clarify the process of PPC formation, it is necessary to establish whether an intrapolymer complex is ever produced during the course of titration. Since the aggregation state of PPC should depend on its concentration, we tried to study the complexation of HSA with KPVS at $V_t/V_t' \leq 0.05$ (corresponding to $C_x \leq 6.30 \times 10^{-6}$ g/mL). Under such conditions, turbidimetric titration is not useful, but SLS and QELS methods are effective.

Figure 10 shows the plots of KC_x/R_θ vs $\sin^2(\theta/2)$ obtained at different C_x. A good linear relationship was observed in each plot (correlation coefficients > 0.99); therefore, $\bar{M}_x$ and R_g can be estimated using eq 8. This estimation is simplified by the observation that the second virial coefficient (5.56×10^{-5} cm^3 mol/g^2) obtained from the Zimm plots in Figure 9 was negligibly small. The results obtained are shown in Figure 11, together with the R_h values determined by QELS. It is found that, at $V_t/V_t' < 0.03$ (i.e., $C_x < 3.78 \times 10^{-6}$ g/mL), the values of $\bar{M}_x$, R_g, and R_h vary linearly with the added amount of KPVS (regression coefficients ≥ 0.99). This variation in size is in contrast to the constant size inferred from turbidimetric titration and QELS, as reported in Figures 2, 3, and 6. The change in size at very low C_x is due to the different states of aggregation of intrapolymer complexes, i.e., variation in α at low C_x. In the range of C_x reported in Figures 2, 3, and 6, aggregates appear to be stable with respect to size and mass (the reason for this will be discussed below). Extrapolation to $C_x \rightarrow 0$ gave limiting values: $\bar{M}_x' = 9.5 \times 10^5$, $R_g' = 32$ nm, and $R_h' = 13$ nm. The obtained value of $\bar{M}_x'$ is in excellent agreement with the calculated $\bar{M}_x^{\circ}$ for an electrically neutral intrapolymer complex ($=\bar{M}_{PE} + (Z_{PE}/Z_{pro})M_{pro}$), providing clear evidence for the formation of intrapolymer PPC. This result is in dramatic contrast to findings for the BSA−poly(diallyldimethylammonium chloride) (PDDA) complex obtained under similar conditions for M_{PE}, M_{pro}, and C_x but in 0.01 M phosphate buffer (pH 7.9).[4,20] In that case, a negatively charged intrapolymer complex with $\bar{M}_x = 8 \times 10^6$, i.e., $\bar{n} = 40$, was found. The tendency of the polymer to bind much less protein in the present case may be ascribed to a tendency toward the formation of electrically neutral complexes in pure water and at high protein charge.

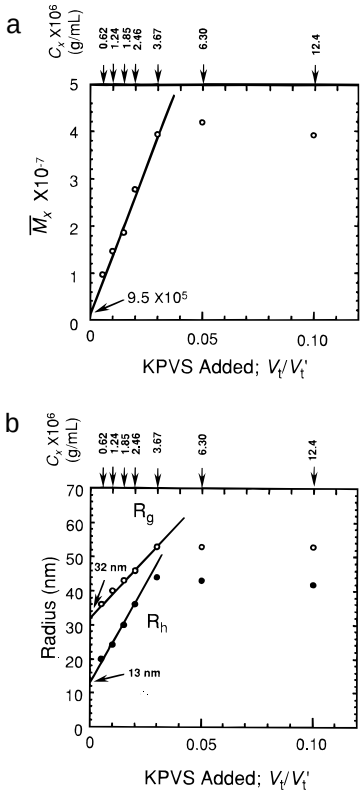

Figure 11. Changes in $\bar{M}_x$ (a), R_g (b), and R_h (b) of a HSA−KPVS complex with different V_t/V_t's.

The values of R_g' and R_h', 32 and 13 nm, respectively, are remarkably close to the values obtained for protein-free KPVS in 0.2 M NaCl, i.e., $R_g = 31$ and $R_h = 12$ nm. The complex thus appears to have a very similar configuration to that of the uncomplexed chain. It would appear that any contraction due to local collapse of polymer segments on the protein surface is compensated for by interprotein steric repulsion.

(31) Konishi, T.; Yoshizaki, T.; Yamakawa, H. *Macromolecules* **1991**, *24*, 5614.

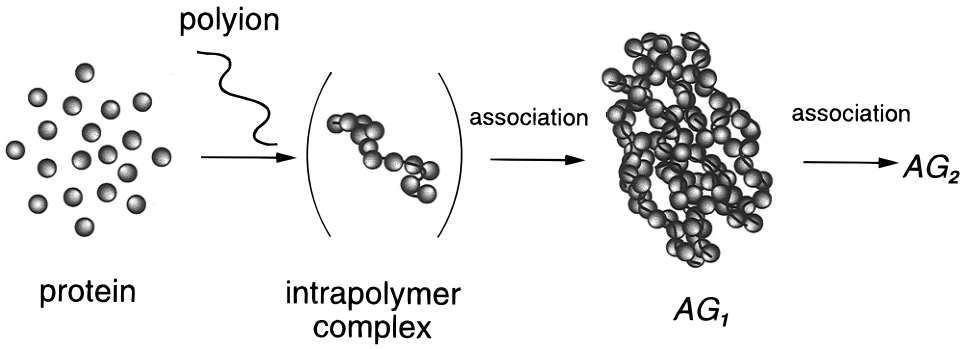

Figure 12. Schematic illustration of processes of PPC formation inferred from the present study.

All of the samples used in SLS and QELS were examined by ELS, from which we found that, even at $V_t/V_t' < 0.02$, the ELS spectra show a discernible shoulder at mobility = 0 μm·cm/V·s (see Figure 7; this shoulder appeared indistinctly in the spectra at $V_t/V_t' = 0.01$ and 0.005). Therefore, we believe that the intrapolymer PPC is neutral, as assumed in the previous section.

IV.9. Mechanism of PPC Formation. The processes of PPC formation inferred from the present study are schematically shown in Figure 12. Upon addition of KPVS to a protein solution, the protein molecules bind to a flexible polyion via Coulomb attraction, resulting in an intrapolymer complex, in which the polyion charges are balanced by protein charges of the opposite sign. The neutral intrapolymer complexes subsequently associate with one another to yield neutral aggregates (AG_1) of a uniform size. Further addition of polyions causes an increase in the concentration of AG_1 without a change in its size. When the AG_1 concentration exceeds a certain level, i.e., $V_t/V_t' > 0.75$, larger aggregates (AG_2) form through association of AG_1. The mechanism of formation needs to be considered, and we also need to explain why the size of AG_1 remains unaltered until the free proteins are nearly consumed. The answers to these questions should help us understand the mechanism of PPC formation.

The spacing between charges on the proteins is not variable and not complementary to the very small and uniform spacing between polymer charges. For this reason, and also from considerations of restrictions on polymer chain configurational entropy, we cannot imagine tight ion pairing in the PPC. Rather, we have to consider the proteins in the PPC as "loosely" bound and the ion pairs as labile and prone to reconfiguration. Furthermore, there must be local regions of excess positive and negative charge. Thus, while the intrapolymer complex may have net electroneutrality, it is highly "polarizable". This polarizability promotes the formation of aggregates of intrapolymer complexes, which we have designated as AG_1. For reasons not completely clear at this time, a relatively well-defined degree of aggregation, i.e. $\alpha \sim 50$, seems to be particularly stable as long as excess protein is present. As the "stoichiometric end point" ($V_t = V_t'$) is approached and free protein is consumed, an abrupt increase in turbidity is observed, signaling the formation of higher-order aggregates, which we designate as AG_2.

For proteins of lower charge density, electrostatic complementarity with KPVS is even more difficult. Furthermore, a large number of proteins must bind to yield an electrically neutral complex. An example is pepsin, for which the requisite number ($\bar{n}$) of proteins is 228. Such an intrapolymer complex would be expected to be quite large, due to steric repulsion among bound proteins. If we envision the polymer chain as "covered" with bound proteins, the formation of higher aggregates might be precluded by intercomplex repulsion. These considerations are consistent with two observations for pepsin PPC: particles of large size (≥280 nm) are formed at low polymer concentration, but turbidimetric titration curves do not show strong scattering. We thus imagine that the pepsin PPC is a highly asymmetric intrapolymer complex of large dimensions but with a mass that is small relative to those of the other PPCs at comparable C_x.

If pepsin PPCs are "covered with" protein, they should interact readily with excess KPVS present at $V_t > V_t'$. We find in fact that negatively charged particles with a size smaller than that of AG_1 are formed under these conditions (see Figures 4b and 8). Similar results were seen when PDDA was added to an aqueous solution containing the neutral PPC of hemoglobin and KPVS.[11]

We would expect to see similar behavior for other proteins with low charge. Experiments carried out with lysozyme at varying pH (Figure 6) support this. Turbidimetric titration curves are seen to resemble those for pepsin as the pH comes close to the isoelectric point for lysozyme.

The formation of aggregates may involve the redistribution of bound proteins, the ease of which may be sensitive to protein surface charge distributions. In general, we expect that proteins of lower surface charge density will form longer-range and therefore more labile ionic bonds than more highly charged proteins and will therefore yield more labile complexes. However, the protein charge density can be quite heterogeneous and the number of charges per unit mass may not in itself control the aggregation state. Thus, proteins of similar charge/mass ratio (similar $\bar{n}$) such as lysozyme, ribonuclease, and trypsin, are observed to have different aggregation states (α is very small for ribonuclease), while proteins with different charge/mass ratios (HSA, papain, lysozyme, and trypsin) may have similar aggregation states.

In conclusion, it appears that, in a salt-free solution, proteins form an intrapolymer complex with strong polyanions through stoichiometric neutralization between opposite charges. The resulting intrapolymer complexes are not particularly stable but instead strongly tend to associate with each other to form aggregates of a uniform size. This association process accompanies the redistribution of the bound proteins, in which the distribution of charges on the protein surface could play an important role and through which the size of aggregated intrapolymer complexes is uniquely determined.

Acknowledgment. We wish to thank K. Mattison of Indiana-Purdue University for his critical reading of this manuscript. This research was supported in part in Japan by a grant to E.K. from the Ministry of Education (#05044077) and in the United States by a grant to P.L.D. from The National Science Foundation (NSF-DMR 9311433), jointly funded by the Divisions of Materials Research and Chemical Transport Systems.

LA960653M